Transduction Efficiency of Adeno-associated Virus Serotypes 2 and 3 Vectors Containing Single- or Double-stranded DNA Genomes

By Frederick Ashby

Bachelor's Degree Student at the College of Agriculture and Life Science:

Microbiology and Cell Sciences/Bioinformatics

Master's Degree Student at the College of Public Health and Health Professions:

Public Health: Policy and Management Specialization

Undergraduate Researcher at the College of Medicine

Pediatrics Department: Cellular and Molecular Therapy

Faculty Advisor: Arun Srivastava, PhD

George H. Kitzman Professor of Genetics and Division Chief

Table of Contents

Abstract	••••••	2
Background	• • • • • • • • • • • • • • • •	3
Materials and Meth	ods	5
Overview		5
MaxiPrep		7
Transfection and V	rus Purification	8
Quantitative Real-	Time PCR Titering	9
Vector Transfectio	n of Human Hepatocarcino	oma Cell Line Huh7 10
Imaging and Quant	tification via Fluorescence	Microscopy 10
Fluorescence Qua	ntification via Flow Cytom	etry 11
Results	• • • • • • • • • • • • • • • • • • • •	
Fluorescence Microscopy		
Flow Cytometry		12
Discussion and Cor	nclusion	
Acknowledgement	S	• • • • • • • • • • • • • • •
Citations	• • • • • • • • • • • • • • • • • • • •	• • • • • • • • • • • • • • • • • • • •
Appendix	••••••	
Contact Information		
Author Frederick Ashby Email: rickv.ashbv@ufl.edu	Principal Investigator Arun Srivastava, PhD Email: aruns@ped.ufl.edu	Lab Manager Chen Ling, PhD Email: lingchen@peds.ufl.edu

Phone: (407) 704-0214 **Phone**: (352) 273-8259 **Phone**: (352) 273-8253

Abstract

Adeno-associated virus (AAV), which naturally contains single-stranded (ss) DNA in its genome, is a non-pathogenic member of the Dependovirus genus, and is widely becoming a revolutionary precision tool in gene therapy. Although ssDNA genomes are transcriptionally-inactive, the development of self-complementary (sc) DNA genomes packaged in AAV vectors have increased the transduction efficiency of AAV2. However, scDNA genomes also reduce the packaging capacity and may elicit more robust immune responses. The transduction efficiency of scDNA within AAV3 capsid serotype, a novel candidate for liver-cancer treatment, has not previously been characterized in comparison to AAV2. In these studies, AAV2 vectors were created with either a ssDNA or scDNA genome (ssAAV2; scAAV2) along with AAV3 equivalents (ssAAV3; scAAV3) containing enhanced GFP reporter gene driven by a chicken-beta-actin promoter. The biological activity of each vector was determined in a human liver cancer cell line (Huh7) using fluorescence microscopy and flow cytometry. Both confirmed there is indeed a significant difference between AAV2 and AAV3 in how they express scDNA versus ssDNA. While AAV2 has significantly higher transduction with self-complementary genomes, AAV3 appears to have little difference between single-strand versus self-complementary. These results provide insight to future clinical vector design and mechanistic discrepancies between vector serotypes.

Background

A member of the Parvoviridae family, AAV does not cause any human diseases and is incapable of replication without the presence of a helper virus. [6] Approximately 4.7kb of single-stranded genomic information is contained within its small capsid. [18] Recombinant AAV (rAAV) vectors are relatively less immunogenic compared to other viral vectors. [6,7] The various serotypes of AAV also have distinctive selective tissue tropism, allowing for specificity in therapeutic gene delivery. [7,8] Various new methods for treating a myriad of diseases, including liver cancer^[8,9] and hemophilia A.^[20] are already being tested in preclinical experimentation. It is estimated that human clinical trials utilizing AAV gene therapies currently number in the hundreds. [11] Five genetic diseases have been successfully treated or cured thus far with AAV gene-therapy in clinical trial. AAV gene-therapy treatments include Leber These successful congenital amaurosis, [21,22,27] a form of genetic blindness, which was confirmed by three independent clinical trials, [23,24,25,26] one of which by Dr. Hauswirth et al. of the University of Florida.^[23] Other AAV clinical trials have confirmed success in treating lipoprotein lipase deficiency, [28] hemophilia B, [31] choroideremia, [22,29] and aromatic L-amino-acid decarboxylase deficiency.[30]

Research has shown that AAV3 has increased transduction efficiency within hepatocellular carcinoma cells with tyrosine mutations that prevent capsid ubiquitination,^[2] refining its potential for treatment of liver cancer. The human hepatocyte growth factor receptor (HGFR) was also discovered to be a co-receptor involved in the

cellular entry of AAV3,^[1] making it a logical choice for a gene-therapy treatment targeting liver cancer. HGFR has been identified as playing a key role in liver cancer,^[14] and has been shown to be significantly up-regulated in hepatocellular carcinoma (HCC) patients.^[13] The specificity of AAV3 with HCC cell lines is likely attributable to this correlation. In regards to novel treatments, researchers have proposed using micro-RNA (miRNA) to treat HCC with AAV3 vectors. miRNA could serve as a suppressor for oncogenes by means of AAV gene-therapy, with considerable proof-of-concept shown via a sequence referred to as miRNA 26-a.^[12] When taken together, it is clear that AAV3 may play an integral role in the future of liver cancer treatment, warranting further investigation into its physiology and efficacy as a medical vector.

Previous experiments with AAV capsids have shown that vectors containing scDNA have increased thermo-stability and transcription-initiation rates compared to similar AAV vectors containing ssDNA.^[3] scAAV vectors are able to bypass second-strand DNA synthesis, which is the major rate-limiting step in transduction within ssAAV vectors.^[17,18] Second-strand DNA synthesis along with transcription may also be dependent on capsid proteins.^[4] These experiments to compare transduction efficiency between ssDNA and scDNA have mostly been done with AAV2 and other serotypes, and have not been done with AAV3.^[3,4] Transduction efficiency of AAV can be affected primarily by receptor-binding efficiency, cellular entry, second-strand DNA synthesis, transcription, and translation of the transgene product. Some of these factors may be affected by capsid modification by mechanisms not yet fully understood. When

considering previous research was able to discover transcription may be inhibited 450-fold from a single missense point-mutation, ^[4] it is possible there is a difference in AAV3 expression behavior (in the context of ssDNA versus scDNA genomes) compared to AAV2 given the fact that there are variations in amino acid sequences between serotypes. This may be significant in the design of future gene therapy clinical trials, especially since previous studies have also shown that scAAV vectors under certain circumstances elicit a more robust immune response compared to their single-stranded equivalent. ^[10] This investigation seeks to answer the question: what is the effect on transduction efficiency in AAV3 when packaging a single-stranded genome versus a double-stranded genome and is this effect different than the effect observed in AAV2?

Materials and Methods

Overview

The vector particles for this experiment were created using the Stratagene AAV protocol. [5] Plasmids for transfection were generated using a standard maxi-preparation procedure and then prepared by PEI-mediated transfection of human embryonic kidney (HEK-293) cell lines. Four distinct vectors of recombinant AAV (rAAV) were generated. A single-stranded (ssDNA) or double-stranded (scDNA) enhanced green-fluorescence protein (eGFP) gene driven by a chicken-beta-actin (CBA) promoter was packaged into one of two capsids: AAV2 or AAV3. Viral titer for each yield of virus subtype was measured by quantitative real-time PCR (qPCR) using a BIORAD MyiQTM Optics Module single-color model with SYBR® Green *Power Mix*. Single- and double-strand

vectors of each capsid serotype were prepared in stock solutions for transfection at an equivalent multiplicity of infection (MOI). The MOI used for these studies was 5,000 viral-genomes per cell for all vectors tested. All vectors were used to transfect the same cell-line, hepatocarcinoma cells (Huh7), which has been previously shown to be competent to both rAAV2 and rAAV3. See **Table 1** for illustrated details.

Table 1	AAV2 Capsid	AAV3 Capsid
ssEGFP w/CBA promoter	ssAAV2	ssAAV3
scEGFP w/CBA promoter	scAAV2	scAAV3

The cells were then observed for fluorescent disparities between ssDNA versus scDNA in each capsid type using flow-cytometry and fluorescent imaging. These discrepancies in fluorescence were used as indirect markers for relative transduction efficiency of each vector, and can, to a very limited degree, be speculated as an inverse measure of second-strand synthesis efficiency.

Statistical analyses were done via Google Sheets and One-Way ANOVA. The standard deviation, population mean, and confidence intervals for each group were determined and analyzed. One-Way ANOVA results were obtained using open-sourced script from "Guerrilla Statistics."^[19] Bonferroni and Tukey-Kramer P-values were compared being interpreted as conservative and non-conservative estimates, respectively. All p-values listed in final results are derived from the Bonferroni model.

The add-on script text that was used is available for use as a PDF at: https://drive.google.com/file/d/0B2iiZt9v2siNVXZ5NIBTS0dYSEE/.

MaxiPrep Protocol

Stock *Escherichia coli* for plasmid cloning was prepared by electroporation transformation of DH5-alpha competent cells. Each plasmid used contained an ampicillin resistance marker gene, and transformed cells were incubated in lysogeny broth (LB) with 1g/L of ampicillin antibiotic at 37°C for 24 hours, plated and screened via Qiagen™ mini-preparation protocol. The purified sample DNA was confirmed via Sanger sequencing. Confirmed strains were cultured in liquid LB (1g/L ampicillin) and frozen at -80°C for long-term storage. LB was prepared at a ratio of 10g NaCl, 5g yeast extract and 10g tryptone per each liter. All LB products were purchased from Fisher Scientific. These strains were then grown in 1L of LB-ampicillin mixture at 37°C while being shaken at 200 RPM in a Thermo™ Electron Forma Shaker for a span of 24-48 hours. The resulting plasmid yield within the culture was purified using the following steps respective to each liter culture:

- 1. Bacterial pellet was resuspended in 20mL modified Tris-EDTA solution (25 mM Tris-HCl, pH 8.0; 10 mM EDTA; 50 mM glucose).
- 2. Lysozyme was added (5mL of 50 mg/ml in Q H₂O Sigma L6876-25G).
- 3. A mixture of 24mL of 2% SDS and 24mL NaOH was added.
- 4. A neutralizing solution of 36mL (4.8pH; 3M sodium acetate) was added with 200µL of chloroform.
- 5. The resulting mixture was centrifuged using a Beckman Coulter Rotor 9.1 at 6,300rpm for 40 minutes at 4°C with deceleration set to low setting.
- 6. Supernatant was transferred and 33mL of 40% PEG was used to precipitate the bacterial chromosome.
- 7. Sample was centrifuged using a Beckman Coulter Rotor 16.25 for 30 m at 10,000rpm and 4°C. Supernatant was discarded and pellet was dissolved in 37
- 8. RNA was precipitated by adding 10mL of 5.5M lithium chloride and centrifuging with a Beckman Coulter Rotor 16.25 for 20 minutes at 10,000rpm and 4°C.
- 9. Supernatant was transferred and 100% ethanol was added at a ratio of 70% of the volume to precipitate plasmid DNA.

- 10. Supernatant-ethanol mix was centrifuged with a Beckman Coulter Rotor 25.5 for 15 minutes at 10,000g at room-temperature. Resulting pellet was dissolved in 8.5mL of Tris-EDTA solution (1% 1M Tris; 0.2% 0.5M EDTA; and 98.8% water by volume) and incubated at 37°C with 5-prime RNase A (lot#142357211) for 40 minutes to eliminate any remaining RNA contamination.
- 11. Plasmid DNA band was extracted on a cesium chloride density gradient with ethidium bromide as a marker. Ethidium bromide was removed from DNA solution by decanting with saturated butanol.
- 12. Cesium chloride was removed from DNA solution by dialysis in hypotonic Tris-EDTA solution, and final DNA concentration ($ng/\mu L$) and purity (A_{260}/A_{280}) was confirmed by Nanodrop lite spectrophotometer. All DNA samples had an A_{260}/A_{280} purity greater than or equal to 1.9. Samples were further confirmed via endonuclease digestion and electrophoresis. Confirmed samples were archived at -80°C until transfection.

Transfection and Virus Purification Protocol

Plasmids were transfected into competent human embryonic kidney cells (HEK-293) grown in modified DMEM (10% fetal bovine serum and 1% penicillin/streptomycin) using a triple plasmid PEI technique. Appropriate amounts of capsid encoding plasmid, genomic plasmid, and a helper plasmid were calculated in conjunction with PEI to form the appropriate PEI-DNA intermediate in an antibiotic and serum-free DMEM medium. This mixture was added to HEK-293 cells and incubated for 18 hours before modified DMEM was replaced to prevent excessive cytotoxicity. The transfected cells were incubated for 72 hours with green fluorescent protein as a marker for transfection efficiency (see **Figure 1**).

Cells were then harvested and centrifuged to discard the medium, and cells were resuspended in 5mL RB TMS buffer. Cell suspension was archived in -80°C storage until viral purification. All virus types compared were made simultaneously to ensure accurate comparison. All procedures involving exposure of samples to open air were done under a biosafety level 2 HEPA filtered hood (SterilGARD® II) that had been UV sterilized prior to use. The virus particles were purified using the following protocol:

Single- or Double-stranded DNA Genomes. University of Florida College of Medicine. 9 April 2015.

- 1. Sample containers were thawed at 37°C, resuspended using Scientific Industries Vortex Genie 2, and refrozen in -80°C 100% ethanol. These steps were repeated 3 additional times to ensure proper cell lysis.
- 2. 1µL of 4.8M MgCl₂ was mixed into each sample.
- 3. 1.2µL of Pierce Universal Nuclease for Cell Lysis (Thermo[™] #88702) was mixed into each sample, then incubated at room-temperature for 1 hour. Samples were vortexed every 10 minutes to ensure proper cell lysis.
- 4. Samples were centrifuged at 3700 rpm for 40 minutes at 4°C. Supernatant was collected for further steps and 10µL crude lysate was aliquoted for qPCR confirmation.
- 5. Virus particles were isolated using an iodixanol step gradient in Beckman 13 mL quick-seal tubes and centrifuged at 73,000 rpm using a 90 Ti rotor in a Optima L-90K Ultracentrifuge at 18°C.
- 6. The 40% iodixanol fraction for each sample was removed and run individually through an Amersham Biosciences flow pump. A HiTrap Q SP column was used to bind AAV2 capsid serotypes, and a HiTrap Q HP column was used to bind AAV3 serotypes. Low and high salt buffers were run through the binding columns prior to each sample in order to ensure clean samples.
- 7. The elution of each sample was collected in Apollo 20mL High-Performance Centrifugal Concentrators (Fisher Science, NC9380552). 10µL crude lysate was aliquoted for qPCR confirmation.
- 8. Samples were centrifuged at 3000 rpm for 10 minutes at 4°C, and 20mL of phosphate buffer solution (PBS) was added to the filter.
- 9. Samples were centrifuged again at 3000 rpm for 10 minutes at 4°C. Viruses were collected by resuspension in 0.5mL PBS applied directly to the filter.
- 10. The 0.5mL of virus containing PBS for each sample was transferred to a respective silicone treated tube and archive in a -80°C freezer until gPCR analysis and subsequent virus infection.

Quantitative Real-Time Polymerase Chain Reaction Titering

In order to titer the virus samples produced, quantitative real-time PCR (qPCR) was utilized by creating a standard curve using free eGFP plasmid as a positive control. The same forward and reverse primers were used for all samples, as they all behave similarly. Zymo Research DNA Clean & Concentrator Kit was used to purify the DNA samples.

- 1. To denature the viral capsid, 40µL of Benzonase (Novagen, 70664) solution with a concentration of 100U/mL was added to each sample and incubated at 37°C for 1 hour.
- 2. 50µL of 200 mM NaOH was added to each tube.
- 3. Samples were incubated at 65°C for 30m, then transferred to ice for 5 minutes.
- 4. 700μL of DNA Binding Buffer was added to each DNA sample and vortexed. Each sample was then transferred to a Zymo-Spin Column in a Collection Tube.
- 5. Samples were centrifuge at 13,000 rpm for approximately 1 minute. Samples were washed with 200µL of 20% Wash Buffer and 80% ethanol solution three times.
- 6. 100μL of 37°C sterile DNase-RNase free H₂O was added directly to the column matrix for elution using the same centrifugation settings listed above.

7. 5 μL of each sample elution was aliquoted to each qPCR tube along with 12.5 μL of Power SYBR® Green PCR Master Mix (Applied Biosystems by Life Technologies #4367659), 6 μL of sterile DNase-RNase free water and 1.5 μL of 10μM solution forward and reverse primers (final primer concentrations 375nm each).

Vector Transfection of Human Hepatocarcinoma Cell-Line Huh7

An Huh7 cell-line was maintained in DMEM with 10% fetal bovine serum and 1% penicillin/streptomycin in a 37°C incubator with a 5% CO₂ atmosphere. These cells were quantified and aliquoted into a 96-well plate in equivalent amounts of 10,000 cells per well. The viral titer obtained from the qPCR results were used to calculate an appropriate dose to achieve an MOI of 5,000vg/cell. Viral inoculation medium was prepared with DMEM without FBS or antibiotics and the appropriate amount of virus suspended in PBS. Cells were then incubated at 37°C with a 5% CO₂ atmosphere before the medium was replaced with modified DMEM (10% FBS and 1% antibiotics).

Imaging and Quantification via Fluorescence Microscopy

Transfected Huh7 fluorescent images were captured approximately 48 hours after initial transfection of viruses. Cells were prepared by replacing DMEM medium with 30µL PBS. Microscopic magnification was done using *Leica DMI 4000B* automated inverted research microscope with an *X-Cite Series 120Q* fluorescent illuminator. Image capturing was done via RT KE/SE SPOT digital camera. Analysis and processing of images were done via ImageJ, an open-source Java based imaging software optimized for research applications.^[32]

Fluorescence Quantification via Flow Cytometry

Flow cytometry was done approximately 72 hours post-transfection via BD Accuri[™] C6 Cytometer model. An equivalent set of wells containing Huh7 cells of equal portions to those transfected was used as a mock group. Samples were washed with PBS and digested with trypsin at 37°C with 5% CO₂ atmosphere for approximately 8 minutes. Cells were resuspended in DMEM, centrifuged, separated from supernatant and then resuspended in modified PBS (2% FBS). The top percentile of fluorescence in the mock group was used as a threshold for GFP detection. The FL1-A fluorescence setting was used with a 488nm laser and a 533/30 filter to detect GFP activity.

Results

Fluorescence Microscopy

The discrepancies between in fluorescence at 48 hours post-transfection of these four vectors are shown in **Figure 2**. Example images of vector transduction efficiency measured by fluorescence microscopy can be seen in **Figure 3** for qualitative analysis. Due to the comparatively immense size of scAAV2 fluorescence in comparison to all other vectors, a logarithmic representation of Figure 3 is shown in **Figure 4**. Fluorescence was seen in AAV2 to be significantly higher in scDNA vectors compared to their ssDNA equivalent vector (p=0.000023). These results are consistent with previous reports, and serve as a valid control group to compare AAV3 expression discrepancies between genome types. Fluorescence in scAAV2 was determined to be approximately 560% higher than in ssAAV2. scAAV3 vectors were shown to not be

significantly higher or lower than their single-stranded equivalent (p=0.26), as determined by One-Way ANOVA analysis. Although, it should be noted that the mean of scAAV3 fluorescence was still calculated to be approximately 63% higher than ssAAV3, despite the lack of significance. The net increase in transduction efficiency of scAAV serotypes compared to their ssAAV equivalent are shown in **Figure 5** and **Figure 6**. Figure 6 is a logarithmic representation of Figure 5, as before, and it should be noted that the negative range of the 99% confidence interval is not detectable. It is apparent from the graphs that AAV2 and AAV3 are significantly disparate from each other in this comparison. Therefore, AAV3 vectors were shown to have a different expression profile of scDNA versus ssDNA genomes when compared to AAV2 (p=0.000013). This rejects the null hypothesis that the expression profile of scDNA vectors in comparison to their ssDNA equivalents are the same between AAV2 and AAV3, and supports the notion that there may be a difference in the intrinsic physiology of how these serotypes facilitate the expression of transgene products.

Flow Cytometry

The fluorescence microscopy results were confirmed via flow cytometry analysis at 72 hours post-transfection. The mean-fluorescence of each sample was determined (see **Figure 7**), and was approximately: 1.212x10⁵ for ssAAV2; 1.775x10⁵ for scAAV2; 7.904x10⁴ for ssAAV3; and 9.057x10⁴ for scAAV3. In reference to the number of cells detected by the flow-cytometer to be in the top percentile of fluorescence within the mock group, the scAAV2 vector group was shown to have 46% increase in mean

fluorescence detected compared to its ssAAV2 equivalent. In comparison, scAAV3 only displayed a 15% increase in mean fluorescence compared to its ssAAV3 equivalent. The total percentage of Huh7 cells detected by flow-cytometry to be expressing eGFP at threshold level (see Figure 8) was: 52.97% for ssAAV2; 74.59% for scAAV2; 31.33% for ssAAV3; and 35.83% for scAAV3. In reference to the number of cells detected by the flow-cytometer to be in the top percentile of fluorescence compared to the total cells detected, scAAV2 vectors were shown to transfect with approximately 41% more cell coverage than its ssAAV2 equivalent. In comparison, scAAV3 vectors only showed 14% more coverage than their ssAAV3 equivalent. The primary flow-cytometry histograms are shown in Figure 9. Collectively, the flow-cytometry results showed a relatively large increase in fluorescence in scAAV2 compared to ssAAV2 and a modest increase in fluorescence in scAAV3 compared to ssAAV2. These results are consistent with the previous fluorescent microscopy results. In both flow-cytometry and fluorescence microscopy analysis, the increase in transduction within scAAV2 compared to ssAAV2 was seen to be 2.8 to 4.1 times greater than the increase in transduction within scAAV3 compared to ssAAV3.

Discussion and Conclusion

While these results support the hypothesis that there is a discrepancy between vector serotypes AAV2 and AAV3 in scDNA/ssDNA expression efficiency, more investigation is required to make conclusions regarding the mechanism by which this occurs. It may be worth considering that AAV3 may be able to somehow bypass or

speed-up steps in ssDNA transduction, or alternatively it may simply be somehow incompatible with the improved efficiency provided by the double-stranded genome. If AAV3 capsid proteins do indeed provide some catalytic advantage that allows packaged single-strand DNA to be expressed with nearly the same efficiency as packaged double-stranded DNA, it may warrant investigating these mechanisms for use in future vectors. This first scenario may lead to the discovery of a method for researchers to produce single-stranded AAV vectors, which have a higher packaging capacity and potentially lower immune response, without sacrificing transduction efficiency that would be gained using a self-complementary alternative. On the other hand, if the situation is caused by AAV3 being somehow unable to exploit the benefit of double-stranded DNA -- which is caused by the bypass of second-strand synthesis, a rate-limiting step of rAAV transduction[17] -- it may be worth investigating what AAV3 is lacking that AAV2 possesses. The second scenario may give future researchers insight into making a double-stranded AAV3 vector, with AAV2-like domains, that is able to more efficiently transduce competent cells. Either of these scenarios are beyond the scope of this study, and are essentially left to speculation until this is investigated.

It should be noted that previous investigations found that scDNA viral genome (double-stranded) titers may be over-estimated using qPCR techniques, [16] and further confirmation of precise viral titers via Southern Blot analysis may yield more confident results. Although, this same study noted that the level of error within wild-type AAV serotypes were modest at best. [16] The fact that the AAV2 fluorescent comparison of

ssDNA versus scDNA in this study is consistent with previous studies may make this systematic error seem unlikely, but not it is certainly not implausible.

In conclusion, the results obtained from this study indicate that scAAV3 have a different effect on transduction efficiency than scAAV2 compared to their respective ssDNA equivalents. Investigation into the mechanisms by which this occurs may yield the discovery of improved methods for designing clinical vectors. The results of these future studies may also provide essential understanding of the biology of AAV itself, along with the differences among various serotypes.

Acknowledgements:

Maria Teresa-Elaine Fajardo-Espinosa-Ashby: For being a dedicated assistant through the transfection process and an amazing individual.

Chen Ling, PhD: For assisting exhaustively throughout the project from start to finish and providing strong foundational training in the procedures required.

Arun Srivastava, PhD: Great success is often made possible by great mentors. Dr. Arun has been one of the best PI's an undergraduate could hope to shadow, and is exemplar of a dedicated researcher.

Jun Li, MD-PhD: For having the patience of a saint in regards to flow-cytometry. Great friends are not always measured by how long you've known them, and Dr. Jun has proven to be a reliable researcher in a very short amount of time.

George Aslanidi, PhD: For expert advice and support throughout the project.

Zifei Yin: For being a friend and a mentor throughout her visit in the United States.

Wenquin Ma & Baozheng Li: For being excellent collaborators and friendly coworkers.

Yuan Hui Zhang: For assisting in procedural modification and optimization.

Daniel Zhang: For being an excellent colleague and friend.

Jayashwi Ramanathan: For giving second opinions about figures and annotations throughout the appendix.

UF Cancer and Genetics Research Complex: For all of the support and the opportunity to learn and serve in a medical research environment that is constructive, innovative, patient-centered and caring for the community.

And all others not named who have invested time and dedication to medical research.

References:

[1]Ling C, Lu Y, Kalsi J, Jayandharan G, Li B, Ma W, Cheng B, Gee S, McGoogan K, Govindasamy L, Zhong L, Agbandje-McKenna M, Srivastava A. Human Hepatocyte Growth Factor Receptor Is a Cellular Coreceptor for Adeno-Associated Virus Serotype 3. *Human Gene Therapy*. Dec 2010; 21(12): 1741–1747.

http://www.ncbi.nlm.nih.gov/pmc/articles/PMC2999576/

^[2]Cheng B, Ling C, Dai Y, Lu Y, Glushakova L, Gee S, McGoogan K, Aslanidi G, Park M, Stacpoole P, Siemann D, Liu C, Srivastava A, Ling C. Development of optimized AAV3 serotype vectors: Mechanism of high-efficiency transduction of human liver cancer cells. *Gene Therapy*. 2012 April; 19(4): 375–384.

http://www.ncbi.nlm.nih.gov/pmc/articles/PMC3519243/

^[3]Horowitz E, Rahman K, Bower B, Dismuke D, Falvo M, Griffith J, Harvey S, Asokan A. Biophysical and Ultrastructural Characterization of Adeno-Associated Virus Capsid Uncoating and Genome Release. *Journal of Virology*. Mar 2013; 87(6): 2994–3002.

http://www.ncbi.nlm.nih.gov/pmc/articles/PMC3592113/

^[4]Salganik M, Aydemir F, Nam H, McKenna R, Agbandje-McKenna M, Muzyczka N. Adeno-Associated Virus Capsid Proteins May Play a Role in Transcription and Second-Strand Synthesis of Recombinant Genomes. *Journal of Virology.* Jan 2014; 88(2): 1071–1079.

http://www.ncbi.nlm.nih.gov/pmc/articles/PMC3911664/

[5] Agilent Technologies, Inc. Manual: AAV Helper-Free System. Revision B. *Stratagene Products Division*. 2010: 21-31. Retrieved from: http://www.chem-agilent.com/pdf/strata/240071.pdf

[6] Zinn E, Vandenberghe LH. Adeno-associated virus: fit to serve. Curr Opin Virol. 2014;8:90-7.

Retrieved from: http://www.ncbi.nlm.nih.gov/pubmed/25128609/

^[7]Hareendran S, Balakrishnan B, Sen D, Kumar S, Srivastava A, Jayandharan GR. Adeno-associated virus (AAV) vectors in gene therapy: immune challenges and strategies to circumvent them. *Rev Med Virol*. 2013;23(6):399-413. Retrieved from: http://onlinelibrary.wiley.com/doi/10.1002/rmv.1762/

[8] Ling C, Lu Y, Cheng B, et al. High-efficiency transduction of liver cancer cells by recombinant adeno-associated virus serotype 3 vectors. *J Vis Exp.* 2011;(49).

Retrieved from: http://www.ncbi.nlm.nih.gov/pmc/articles/PMC3197307/

^[9]Ling C, Wang Y, Zhang Y, et al. Selective In Vivo Targeting of Human Liver Tumors by Optimized AAV3 Vectors in a Murine Xenograft Model. *Hum Gene Ther.* 2014;25(12):1023-34.

Retrieved from: http://www.ncbi.nlm.nih.gov/pubmed/25296041

[10]Rogers GL, Martino AT, Zolotukhin I, Ertl HC, Herzog RW. Role of the vector genome and underlying factor IX mutation in immune responses to AAV gene therapy for hemophilia B. *J Transl Med*. 2014;12:25.

Retrieved from: http://www.ncbi.nlm.nih.gov/pmc/articles/PMC3904690/

[11]Pleticha J, Heilmann LF, Evans CH, Asokan A, Samulski RJ, Beutler AS. Preclinical toxicity evaluation of AAV for pain: evidence from human AAV studies and from the pharmacology of analgesic drugs. *Mol Pain*. 2014;10(1):54. Retrieved from: http://www.molecularpain.com/content/10/1/54

[12]Yang X, Zhang XF, Lu X, et al. MicroRNA-26a suppresses angiogenesis in human hepatocellular carcinoma by targeting hepatocyte growth factor-cMet pathway. *Hepatology*. 2014;59(5):1874-85.

 $Retrieved \ from: \ \underline{http://www.ncbi.nlm.nih.gov/pubmed/24259426}$

[13] Karabulut S, Tas F, Akyüz F, et al. Clinical significance of serum hepatocyte growth factor (HGF) levels in hepatocellular carcinoma. *Tumour Biol.* 2014;35(3):2327-33.

Retrieved from: http://www.ncbi.nlm.nih.gov/pubmed/24142532

[14]Yu G, Jing Y, Kou X, et al. Hepatic stellate cells secreted hepatocyte growth factor contributes to the chemoresistance of hepatocellular carcinoma. *PLoS ONE*. 2013;8(9):e73312.

Retrieved from: http://www.ncbi.nlm.nih.gov/pubmed/24023859

- [15]Glushakova LG, Lisankie MJ, Eruslanov EB, et al. AAV3-mediated transfer and expression of the pyruvate dehydrogenase E1 alpha subunit gene causes metabolic remodeling and apoptosis of human liver cancer cells. *Mol Genet Metab*. 2009;98(3):289-99. Retrieved from: http://www.ncbi.nlm.nih.gov/pubmed/19586787
- [16]Wang Y, Ling C, Song L, et al. Limitations of encapsidation of recombinant self-complementary adeno-associated viral genomes in different serotype capsids and their quantitation. *Hum Gene Ther Methods*. 2012;23(4):225-33. Retrieved from: http://www.ncbi.nlm.nih.gov/pubmed/22966785
- ^[17]Ferrari FK, Samulski T, Shenk T, Samulski RJ. Second-strand synthesis is a rate-limiting step for efficient transduction by recombinant adeno-associated virus vectors. *J Virol*. 1996;70(5):3227-34. Retrieved from: http://www.ncbi.nlm.nih.gov/pubmed/8627803
- [18]Le bec C, Douar AM. Gene therapy progress and prospects--vectorology: design and production of expression cassettes in AAV vectors. *Gene Ther*. 2006;13(10):805-13. Retrieved from: http://www.nature.com/gt/journal/v13/n10/full/3302724a.html
- [19]Guerrella Statistics. Statistics scripts for google docs. *Google Documents Public Access*. Last retrieved April 2015. Retrieved from: https://docs.google.com/document/d/1WFO6k8BaE2Toni41SFeuJ0-ch47AoBTnMYdKCTUdLQE/pub
- ^[20]Wang Q, Dong B, Firrman J, et al. Efficient production of dual recombinant adeno-associated viral vectors for factor VIII delivery. *Hum Gene Ther Methods*. 2014;25(4):261-8. Retrieved from: http://www.ncbi.nlm.nih.gov/pubmed/25093498
- ^[21]Stein L, Roy K, Lei L, Kaushal S. Clinical gene therapy for the treatment of RPE65-associated Leber congenital amaurosis. *Expert Opin Biol Ther*. 2011;11(3):429-39. Retrieved from: http://www.ncbi.nlm.nih.gov/pubmed/21299439
- [22]Carvalho LS, Vandenberghe LH. Promising and delivering gene therapies for vision loss. *Vision Res.* 2014. Retrieved from: http://www.ncbi.nlm.nih.gov/pubmed/25094052
- | E²³| Hauswirth WW, Aleman TS, Kaushal S, et al. Treatment of leber congenital amaurosis due to RPE65 mutations by ocular subretinal injection of adeno-associated virus gene vector: short-term results of a phase I trial. *Hum Gene Ther*. 2008;19(10):979-90. Retrieved from: http://online.liebertpub.com/doi/abs/10.1089/hum.2008.107
- [24]Bainbridge JW, Smith AJ, Barker SS, et al. Effect of gene therapy on visual function in Leber's congenital amaurosis. *N Engl J Med*. 2008;358(21):2231-9. Retrieved from: http://dx.doi.org/10.1056/NEJMoa0802268
- ^[25]Cideciyan AV, Aleman TS, Boye SL, et al. Human gene therapy for RPE65 isomerase deficiency activates the retinoid cycle of vision but with slow rod kinetics. *Proc Natl Acad Sci USA*. 2008;105(39):15112-7. Retrieved from: http://dx.doi.org/10.1073/pnas.0807027105
- [26]Maguire AM, Simonelli F, Pierce EA, et al. Safety and efficacy of gene transfer for Leber's congenital amaurosis. *N Engl J Med.* 2008;358(21):2240-8. Retrieved from: http://dx.doi.org/10.1056/NEJMoa0802315
- [27]Pierce EA, Bennett J. The Status of RPE65 Gene Therapy Trials: Safety and Efficacy. *Cold Spring Harb Perspect Med.* 2015. Retrieved from: http://www.ncbi.nlm.nih.gov/pubmed/25635059
- [28] Gaudet D, Méthot J, Kastelein J. Gene therapy for lipoprotein lipase deficiency. *Curr Opin Lipidol*. 2012;23(4):310-20. Retrieved from: http://www.ncbi.nlm.nih.gov/pubmed/22691709
- [29]Maclaren RE, Groppe M, Barnard AR, et al. Retinal gene therapy in patients with choroideremia: initial findings from a phase 1/2 clinical trial. *Lancet*. 2014;383(9923):1129-37. Retrieved from: http://dx.doi.org/10.1016/S0140-6736(13)62117-0
- [30]Hwu WL, Muramatsu S, Tseng SH, et al. Gene therapy for aromatic L-amino acid decarboxylase deficiency. *Sci Transl Med.* 2012;4(134):134ra61. Retrieved from:http://stm.sciencemag.org/content/4/134/134ra61.long
- [31]Nathwani AC, Tuddenham EG, Rangarajan S, et al. Adenovirus-associated virus vector-mediated gene transfer in hemophilia B. *N Engl J Med.* 2011;365(25):2357-65. Retrieved from: http://www.ncbi.nlm.nih.gov/pubmed/22149959
- [32] Schneider CA, Rasband WS, Eliceiri KW. NIH Image to ImageJ: 25 years of image analysis. *Nat Methods*. 2012;9(7):671-5. Retrieved from: http://www.ncbi.nlm.nih.gov/pubmed/22930834

Tables and Figures

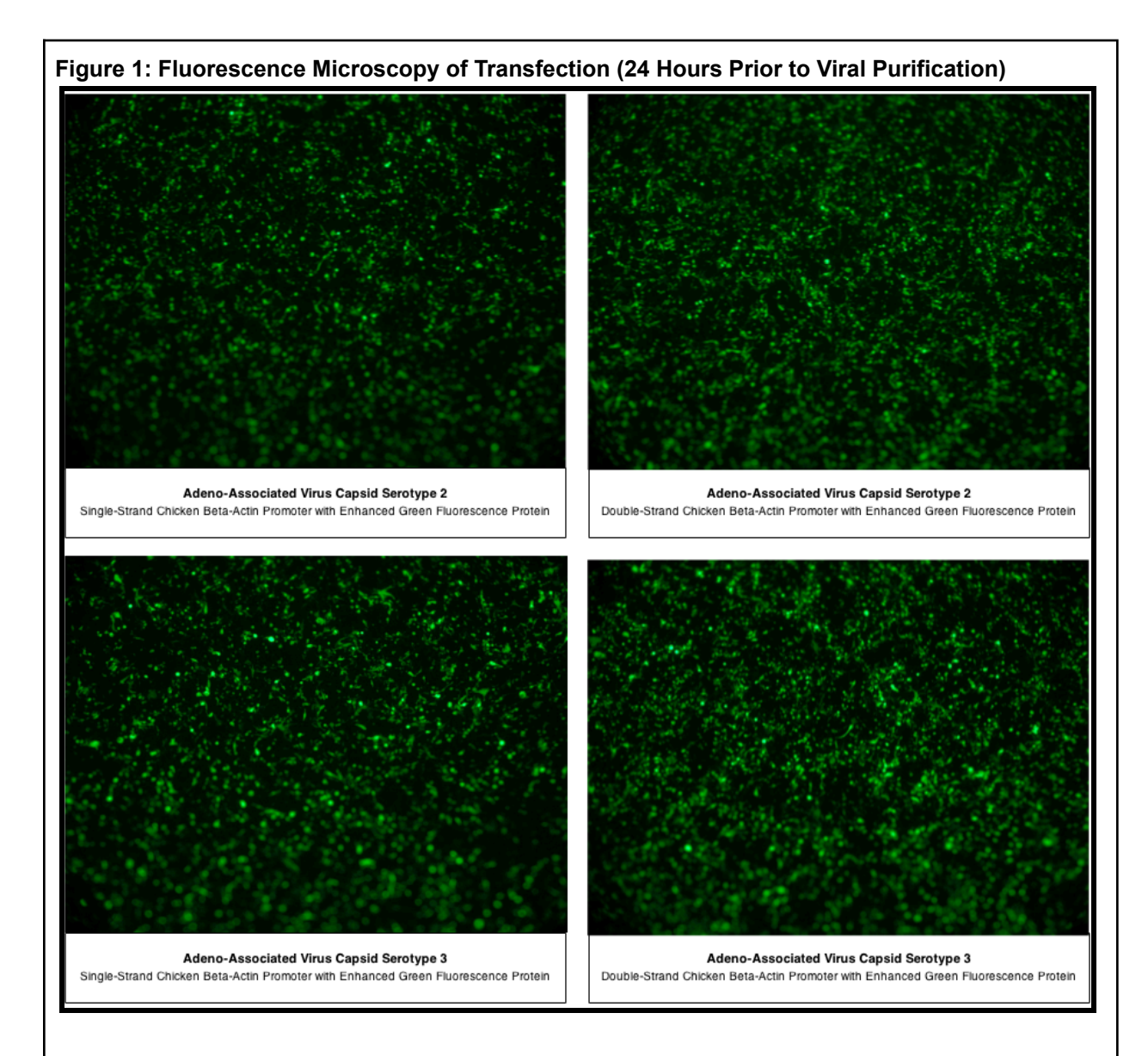


Figure 1: Fluorescence microscopy of 48 hours post-transfection expression of eGFP within HEK293 cells for each vector type. Viruses were harvested 24 hours later and purified using techniques described in *Materials and Methods*.

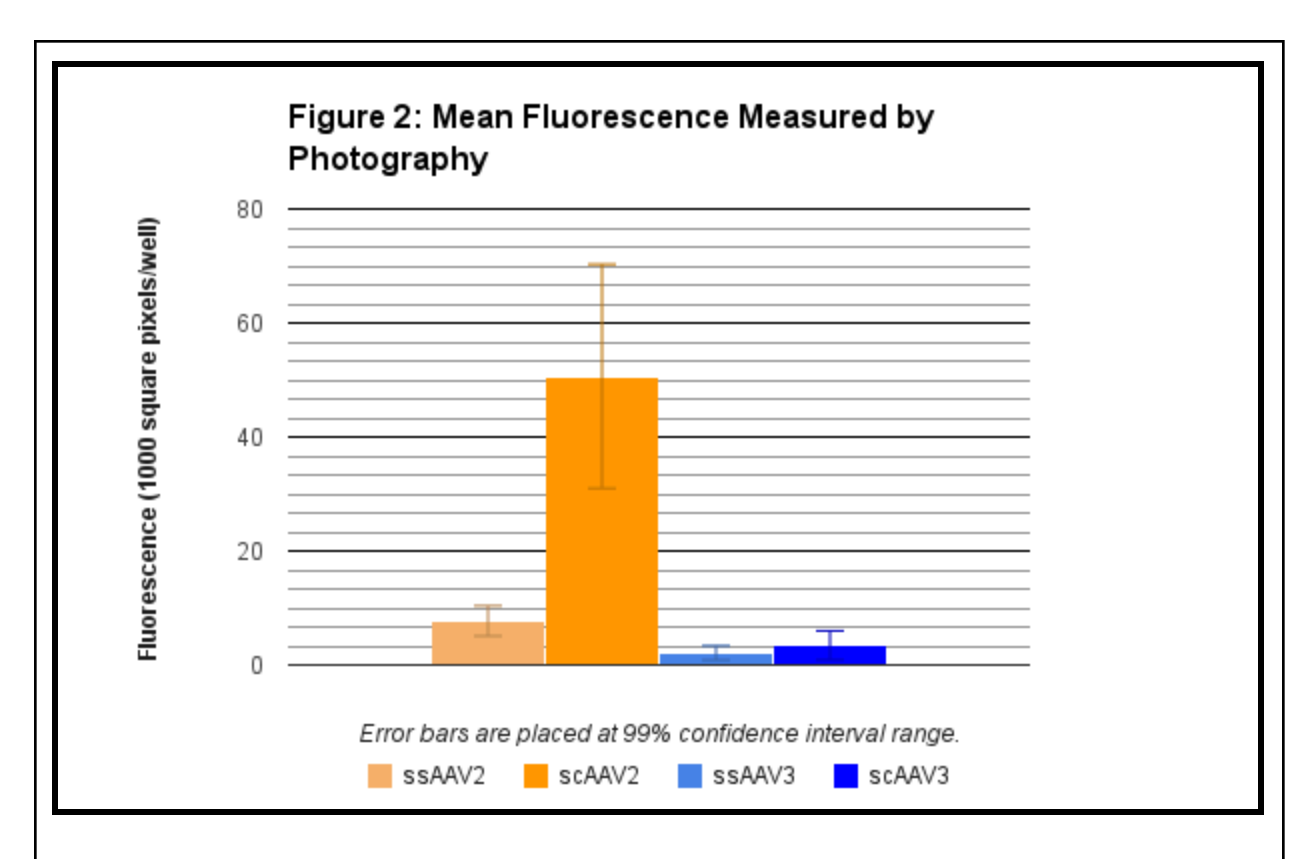


Figure 2: The quantity of mean fluorescence measured by fluorescence microscopy for ssAAV2; scAAV2; ssAAV3; and scAAV3 is shown above with the respective 99% confidence interval range. The fluorescence is measured as 10³ pixels²/well. Significant difference was shown between ssAAV2 and scAAV2 (p=0.000023), however no significant difference was shown between ssAAV3 and scAAV3 (p=0.26).

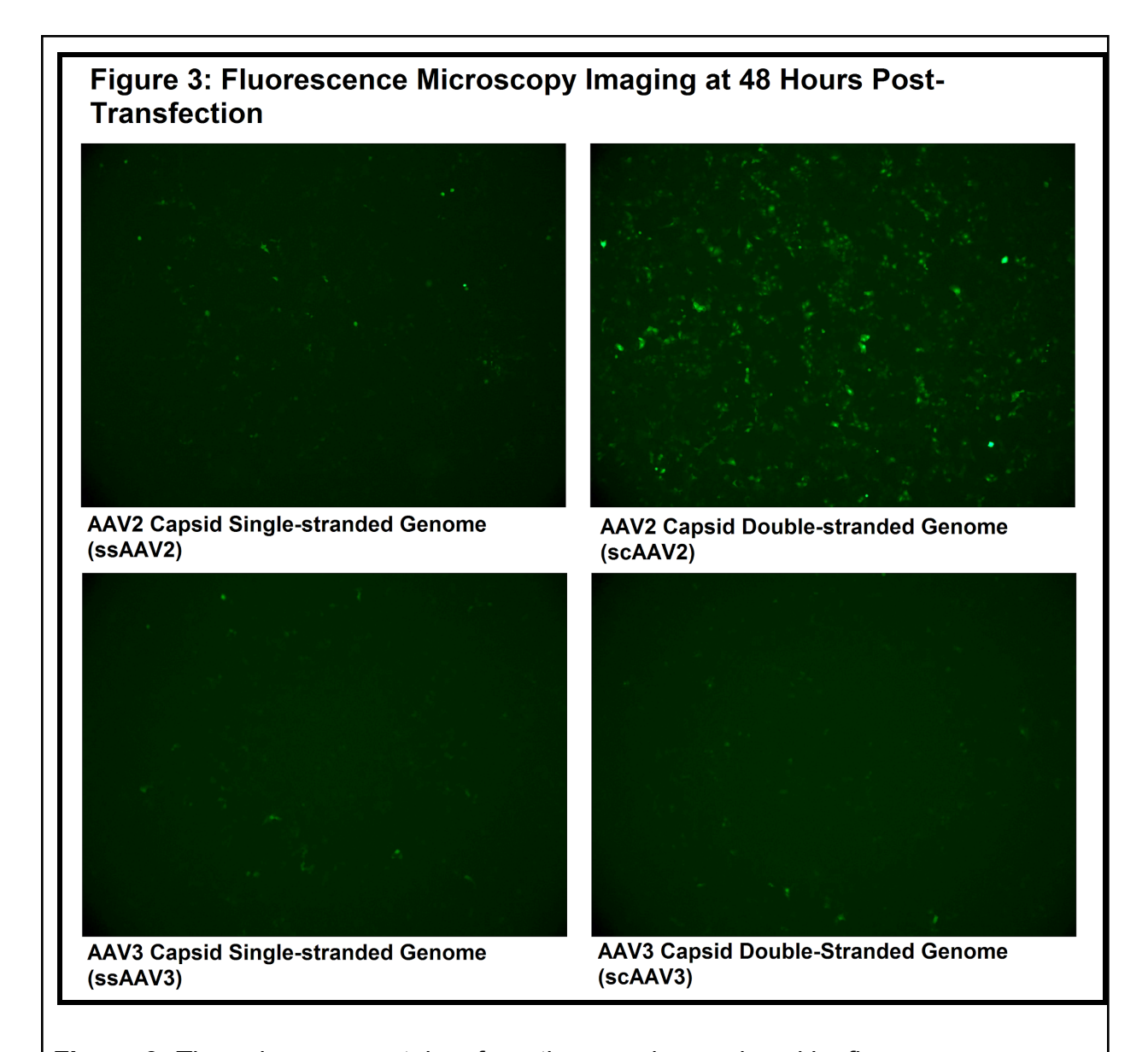


Figure 3: These images are taken from the samples analyzed by fluorescence microscopy. Although there was considerable variation between wells, some statistically confident results were obtained (as illustrated in **Figure 2** and **Figure 4**).

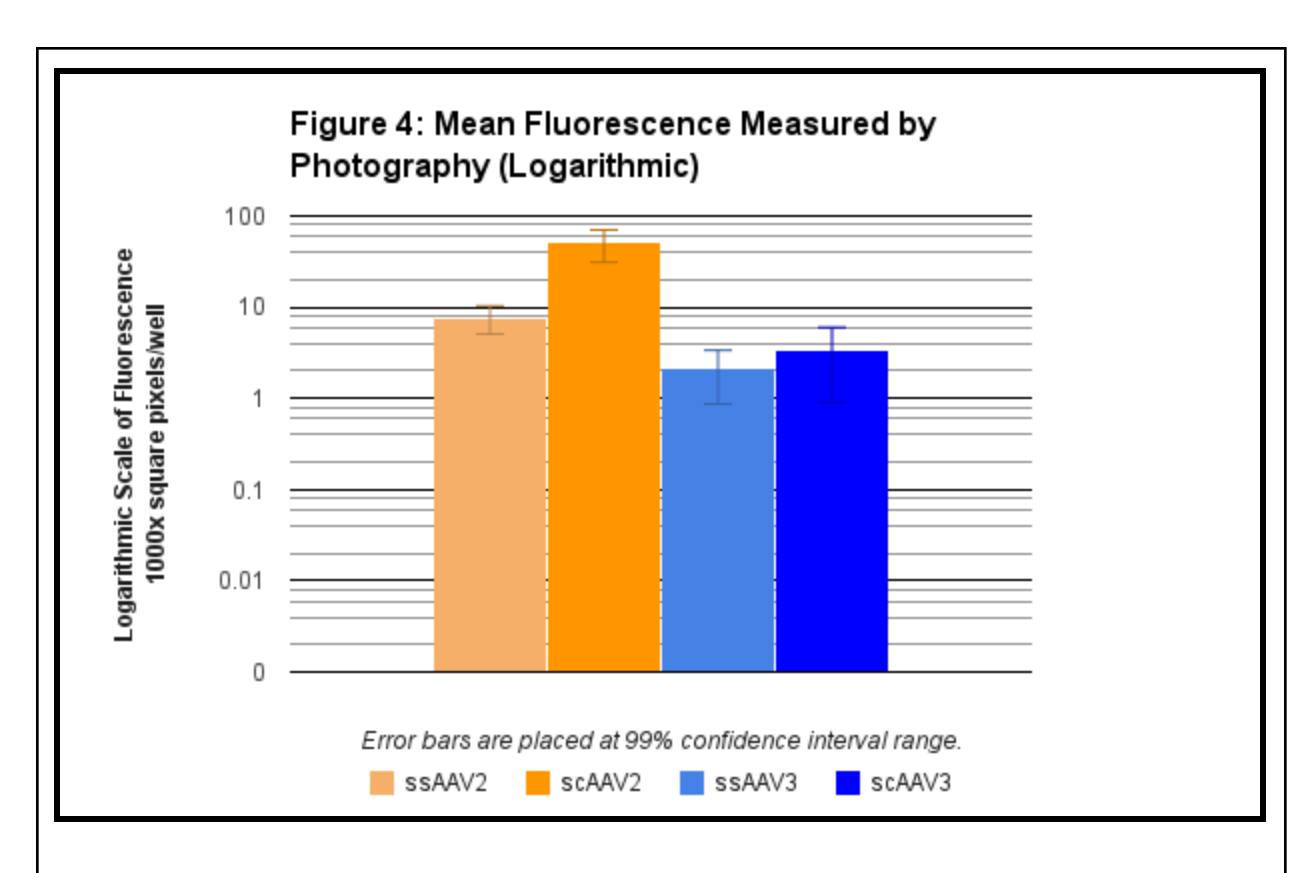


Figure 4: This graph is a logarithmic representation of Figure 2.The quantity of mean fluorescence measured by fluorescence microscopy for ssAAV2; scAAV2; ssAAV3; and scAAV3 is shown above with the respective 99% confidence interval range. The fluorescence is measured as 10³ pixels²/well. Significant difference was shown between ssAAV2 and scAAV2 (p=0.000023), however no significant difference was shown between ssAAV3 and scAAV3 (p=0.26).

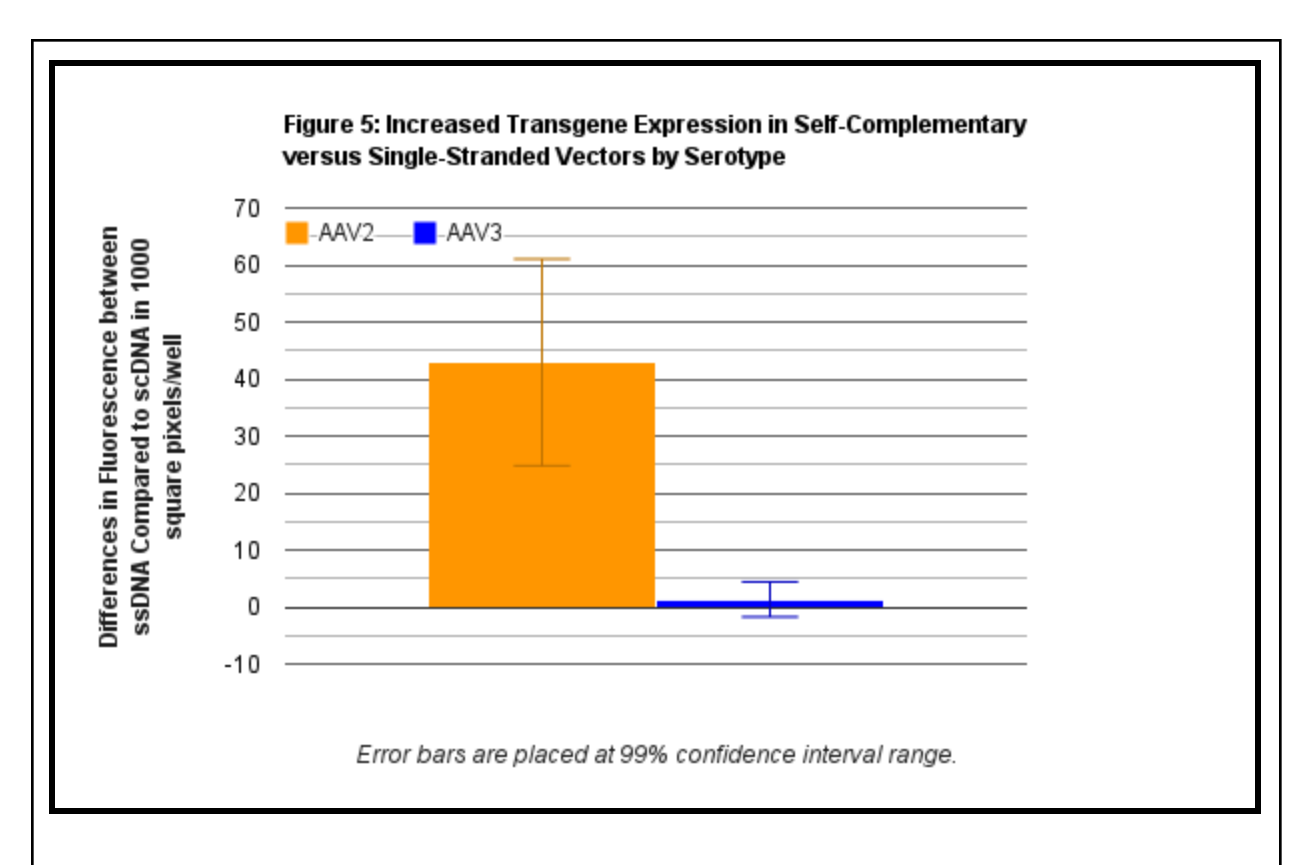


Figure 5: The average difference between ssDNA and scDNA transgene expression in each serotype was calculated and is shown above with the respective 99% confidence interval range. This was obtained directly from fluorescence data measured by fluorescence microscopy. This more clearly illustrates the disparities between serotypes in scDNA versus ssDNA expression. AAV2 serotype had an average increase in transduction efficiency due to scDNA that was significantly higher than the increase in transduction efficiency due to scDNA in AAV3 (p=0.000013). As also illustrated in **Figure 2** and **Figure 4**, the transduction efficiency of scAAV3 was not shown to be significantly higher than ssAAV3 (p=0.26).

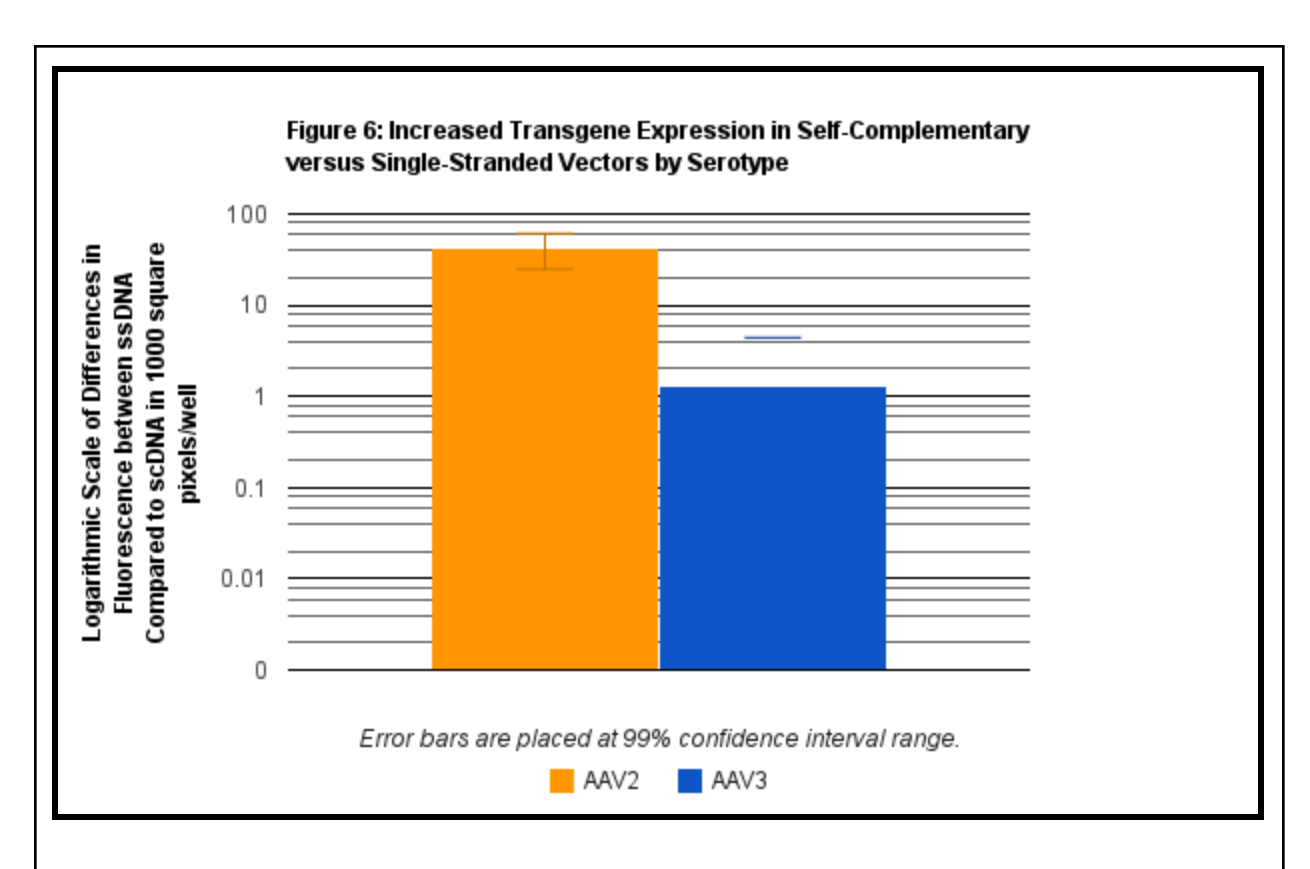


Figure 6: This is a logarithmic representation of Figure 5. The average difference between ssDNA and scDNA transgene expression in each serotype was calculated and is shown above with the respective 99% confidence interval range. This was obtained directly from fluorescence data measured by fluorescence microscopy. This more clearly illustrates the disparities between serotypes in scDNA versus ssDNA expression. AAV2 serotype had an average increase in transduction efficiency due to scDNA that was significantly higher than the increase in transduction efficiency due to scDNA in AAV3 (p=0.000013). As also illustrated in **Figure 2** and **Figure 4**, the transduction efficiency of scAAV3 was not shown to be significantly higher than ssAAV3 (p=0.26).

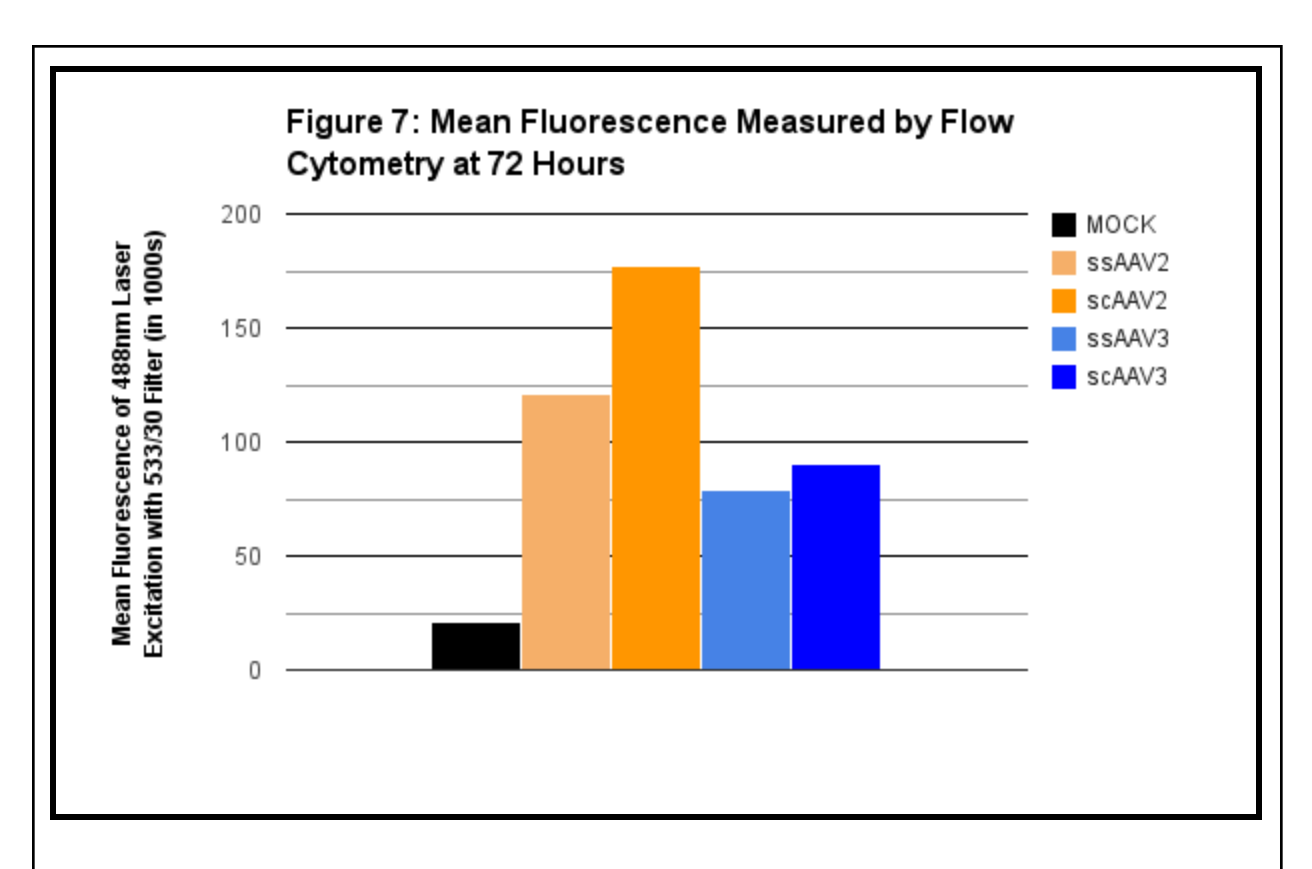


Figure 7: The mean fluorescence as measured by a BD Accuri[™] C6 flow cytometer at 72 hours post-transfection for each vector type is shown above. The excitation wavelength was set to 488nm and the filter was set to 533nm with a range of 30nm. A mock group was used for control which represents a sample of Huh7 cells not transfected by any vector, yet incubated under the same conditions as all other samples for the same amount of time. The fluorescence threshold was measured based off of the top percentile of fluorescence in the mock group. scAAV2 was shown to have 46.39% higher mean fluorescence than its ssAAV2 equivalent. Comparatively, scAAV3 was shown to have a 14.59% increase in mean fluorescence than its ssAAV3 equivalent.

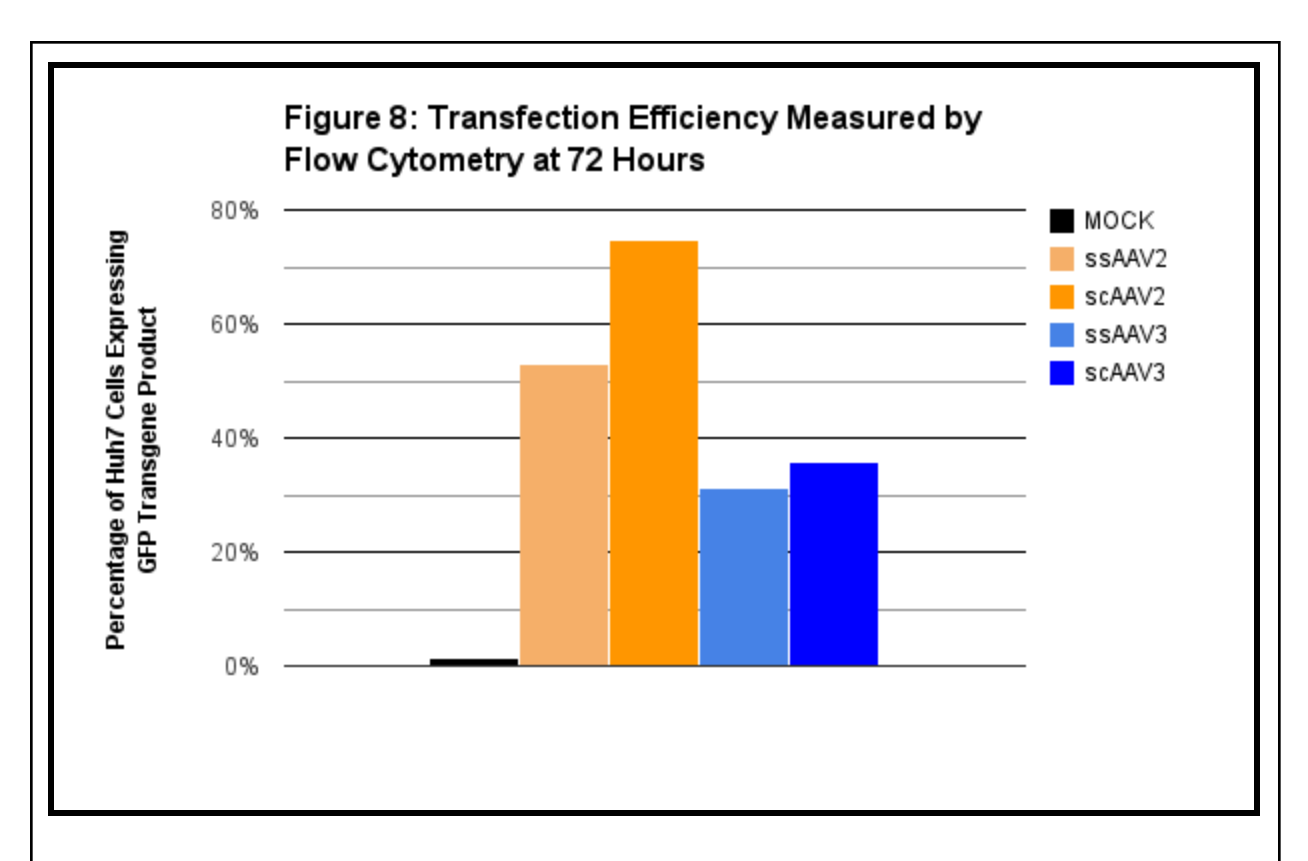


Figure 8: The percent cell transfection coverage as measured by BD Accuri[™] C6 flow cytometer at 72 hours post-transfection for each vector type is shown above. The excitation wavelength was set to 488nm and the filter was set to 533nm with a range of 30nm. A mock group was used for control which represents a sample of Huh7 cells not transfected by any vector, yet incubated under the same conditions as all other samples for the same amount of time. The fluorescence threshold was measured based off of the top percentile of fluorescence in the mock group. The percentage of cells that meet this top percentile threshold were quantified as a percent of the total cells detected. scAAV2 was shown to have 40.08% higher transfection coverage than its ssAAV2 equivalent. Comparatively, scAAV3 was shown to have a 14.36% increase in transfection coverage than its ssAAV3 equivalent.

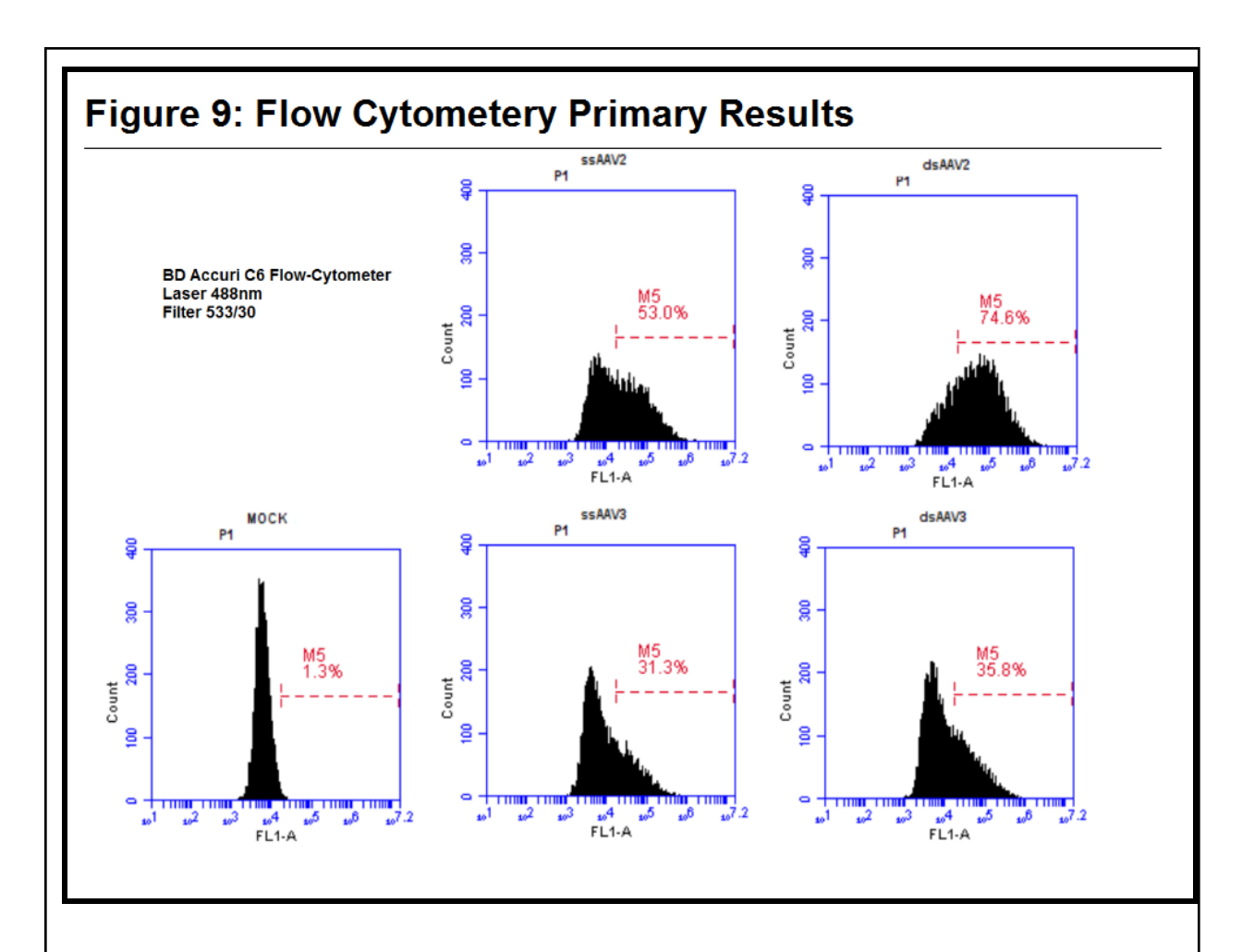


Figure 9: The primary data from the flow cytometer is shown in the figure above, where the M5 range represents the threshold range. Only cells emitting fluorescence within the M5 range are counted for the purposes of analyzing mean fluorescence, omitting non-transfected cells from being misclassified as false-positives.